DEFORMATION AND DEGRADATION STUDY USING POINT CLOUDS IN *NATATIO* OF THE WESTERN BATHS AT *LA ALCUDIA* IN ELCHE (ALICANTE)

ESTUDIO DE DEFORMACIONES Y DEGRADACIONES MEDIANTE EL USO DE NUBES DE PUNTOS EN LA NATATIO DE LAS TERMAS OCCIDENTALES DE LA ALCUDIA EN ELCHE (ALICANTE)

José Antonio Huesca-Tortosa[a,*] , María del Rosario Pacheco-Mateo[b] , Mercedes Tendero-Porras[c] , David Torregrosa-Fuentes[d] , Yolanda Spairani-Berrio[a]

[a] Department of Architectural Constructions, University of Alicante, Carretera de San Vicente del Raspeig, s/n, 03690 San Vicente del Raspeig, Spain. ja.huesca@ua.es; yolanda.spairani@ua.es

[b] PhD Student, University of Alicante, Carretera de San Vicente del Raspeig, s/n, 03690 San Vicente del Raspeig, Spain. mariapachecomateo@gmail.com

[c] La Alcudia Foundation, University of Alicante, Carretera de San Vicente del Raspeig, s/n, 03690 San Vicente del Raspeig, Spain. mercedes.tendero@ua.es

[d] Arquitect, Spain. dtfuentes@hotmail.com

Highlights:

- The current *natatio* of the Western Baths is the result of two different constructive actions/stages.

- The *natatio* suffered deformations and cracks due to differential settlement, which led to its abandonment towards the end of the third century.

- The comparison of the 2016 and 2022 point clouds has allowed the quantification of the increase in deformations and degradations in the *natatio*.

Abstract:

This paper deals with the study of construction and geometry, as well as with the analysis of deformations and active degradations of the *natatio* belonging to the Western Baths in La Alcudia archaeological site. Its location in Elche-Alicante, Spain (Colonia *Iulia Ilici Augusta*), is widely known for the discovery of The Lady of Elche in 1897. The dimensions of this *natatio* in the *frigidarium* are 6.60 x 9.30 m (22 x 31 Roman feet) and 1.50 m deep, making it one of the largest Roman swimming pools documented to date on the Iberian Peninsula. The *natatio* has several cracks sealed with materials used in earlier interventions at the end of the third century. Its comparison with the hypothetical original form allowed the researchers to quantify the current deformations. A damage evolution study has been made comparing the 2016 point cloud with the 2022 cloud, both obtained by light detection and ranging (LIDAR). There is evidence that an active process of degradation and deformation is gradually increasing damage to the pool. By studying the geometry and constructive systems of the *natatio*, relevant data to understand the historical evolution of the Western Baths have been provided. A results analysis conclusion is that the pool was built in two different stages. The eastern half corresponds to the original *natatio*, while the western half was extended or rebuilt after having collapsed. The early abandonment of the use of the *natatio* was most likely due to deformations caused by differential settlement; this occurred when the western half was cemented on landfill between the ancient wall and that of the last third of the 1st century AD.

Keywords: virtual archaeology; Roman *natatio*; diagnosis of cultural damage; terrestrial laser scanning; Colonia *Iulia Ilici Augusta*

Resumen:

El presente trabajo aborda el estudio de la construcción y geometría, así como el análisis de las deformaciones y degradaciones activas que presenta la *natatio* perteneciente a las Termas Occidentales del yacimiento arqueológico de La Alcudia, en Elche, Alicante (Colonia *Iulia Ilici Augusta*); éste es conocido internacionalmente por el hallazgo de la Dama de Elche en 1897. Las dimensiones de esta *natatio* del frigidarium, 6.60 x 9.30 m (22 x 31 pies romanos) y 1.50 m de profundidad, la convierten en una de las piscinas para baños fríos de época romana más grandes de las documentadas hasta la fecha en toda la península Ibérica. La *natatio* presenta varias grietas selladas con materiales empleados en intervenciones anteriores a finales del siglo III. Los resultados obtenidos al realizar el estudio comparativo con su hipotética

---

forma original han permitido cuantificar sus deformaciones actuales. Se ha realizado un estudio de evolución de daños comparando la nube de puntos obtenida en el año 2016 con la nube realizada en el año 2022, ambas obtenidas mediante LIDAR (*light detection and ranging*). Se ha evidenciado que existen degradaciones y deformaciones activas que paulatinamente van aumentando los daños en la *natatio*. El estudio de la geometría y de los sistemas constructivos de la *natatio* también han aportado datos relevantes para la comprensión de la evolución histórica del conjunto de las Termas Occidentales. Del análisis de los resultados de este estudio se concluye que la actual *natatio* se construyó en dos fases diferentes. La mitad oriental coincide con la *natatio* original y la mitad occidental se amplió o se reconstruyó tras arruinarse. El temprano abandono del uso de la *natatio* se debió, con toda probabilidad, a las deformaciones provocadas por asientos diferenciales al cimentar la mitad occidental sobre terrenos de relleno entre la muralla antigua y la del último tercio del siglo I.

Palabras clave: arqueología virtual; *natatio* romana; diagnóstico de construcciones patrimoniales; escáner láser terrestre; Colonia *Iulia Ilici Augusta*

1. Introduction

1.1. The Western Bath at La Alcudia site

After the Roman conquest of the Iberian Peninsula and the territorial reorganization implemented by Rome, a new city that articulates a wide space in the southeast of Spain was founded: *Ilici*. Located next to Via Augusta and culturally and commercially opened to the Mediterranean by the *Portus Ilicitanus* (Santa Pola), it became the most important urban centre between Valentia (Valencia) and *Carthago Nova* (Cartagena). Around the year 26 BC, Ilici was granted the status of colonia by Augustus, the highest rank of a city under Roman law. Over time, it consolidated as a remarkable city, with privileges such as *immunitas* and *ius Italicum*[1] (Alföldy, 2003). Its archaeological remains are today in La Alcudia, site known for the discovery of the Lady of Elche (Abad &Tendero, 2008).

Figure 1: Location of the *natatio*; a) the area within the territory of Elche; b) Orthophoto of the *natatio* and its immediate surroundings; c) Situation of the *natatio* within the archaeological site of La Alcudia.

---

[1] The *inmunitas* granted exemption from all or part of the payment of taxes, and *ius Italicum*, or Italic law, was an honour granted exceptionally by the emperor to certain cities, giving their citizens the same legal status as the inhabitants of Rome.
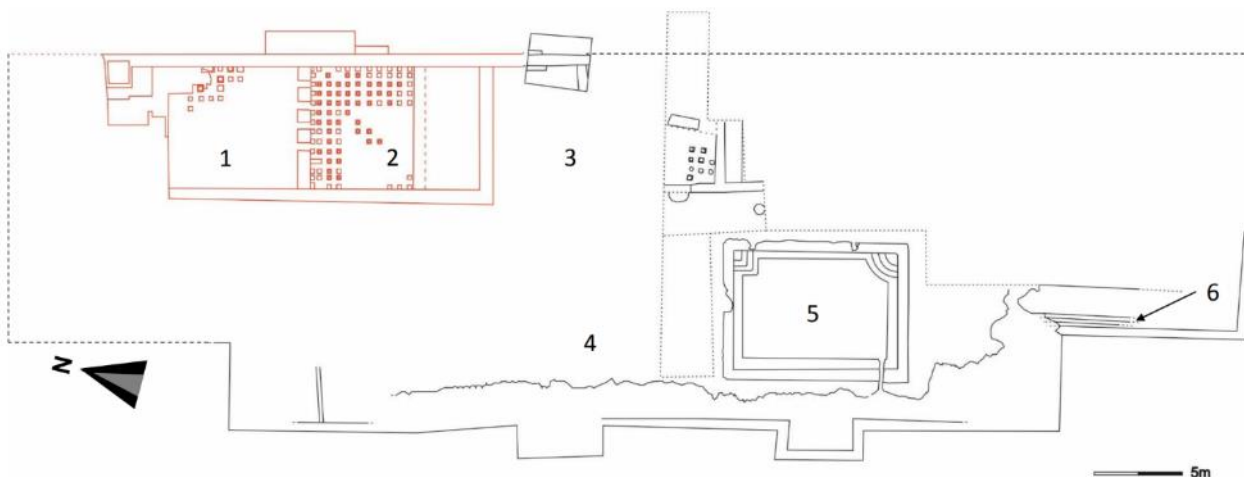
Figure 2: Plan of the Western Baths excavations: 1. Caldarium; 2. Tepidarium; 3. Other units; 4. Frigidarium; 5. Natatio; 6. Specus.

On the western edge of the ancient Colonia *Iulia Ilici Augusta* (Fig. 1), the construction of public urban baths was planned from the extension of the urban perimeter; this event took place in the last third of the 1st century.

For this monumental project, part of the elevation of the city wall, which was built between 30 and 20 BC, was demolished and a portion of the new building was constructed on it.

The result was the expansion of the urban area towards the west and the occupation of an area outside the city. This area was characterized by a steep slope identified by a ditch, which together with the wall, would be part of the defensive system of the city. The western boundary of the baths was projected as a wall stretching more than 60 linear metres where two quadrangular structures were brought forward as buttresses, simulating the appearance of a section of the wall that was then included as part of the foundation of the new building (Tendero & Ronda, 2020).

The Western Baths of *Ilici* (Fig. 2) are now partially excavated. Its estimated perimeter walls delimit an internal space of about 1500 m² in which three different areas can be intuited: one heated, *caldarium*, with an underground chamber through which hot air from an adjacent furnace would circulate; another tempered, *tepidarium*, connected with the previous room by the subsoil, and a large space without heat supply infrastructure, *frigidarium*, which has different rooms, and a large open space that is dominated by a *natatio*.

It should be noted that other thermal complexes are documented in the same archaeological site, both in sector 4C, (Tendero & Ramos, 2014) which was subject to regular excavations and intense plundering in the 5th century, as in 7F (shown in Fig. 1c). The latter, known as *Termas Orientales*, have a slightly larger *natatio*, 10.95 m long and 7.90 m wide (Ramos & Ramos, 2007; Molina, Álvarez & Muñoz, 2018; Álvarez, Molina & Muñoz, 2020; Molina, Muñoz & Álvarez 2020).

The *natatio* under study (Fig. 3) is a work of special relevance. Its dimensions, 6.60 x 9.30 m (22 x 31 Roman feet) and 1.50 m deep (5 Roman feet), make it one of the largest swimming pools for bathing in the Roman period documented to date in the entire Iberian Peninsula (Noguera, García-Entero & Pavía, 2020; Morillo, Durán & García, 2019), with a capacity of approximately 90 m³ of water. Water would be supplied by canals and a possible

aqueduct fed by the River Vinapoló, its channel lying about 500 m to the west. Attached inside the west wall of the baths, there is a section of the *specus* or channel through which water would flow by gravity and it is well preserved.

The *natatio* has two stairways of three steps. Its shape is unique for this kind of constructive element. In the northeast corner, the stairs have a quadrangular form and, in the southeast, the stairs are shaped like a circular segment. This would facilitate the immersion for users and even allow them to sit on the steps.

At the bottom of the *natatio,* there is a continuous bench surrounding its perimeter, which is very common in this type of construction (Noguera et al., 2020). Archaeological studies have proven that this *natatio* must have been in use for several centuries. The *natatio*
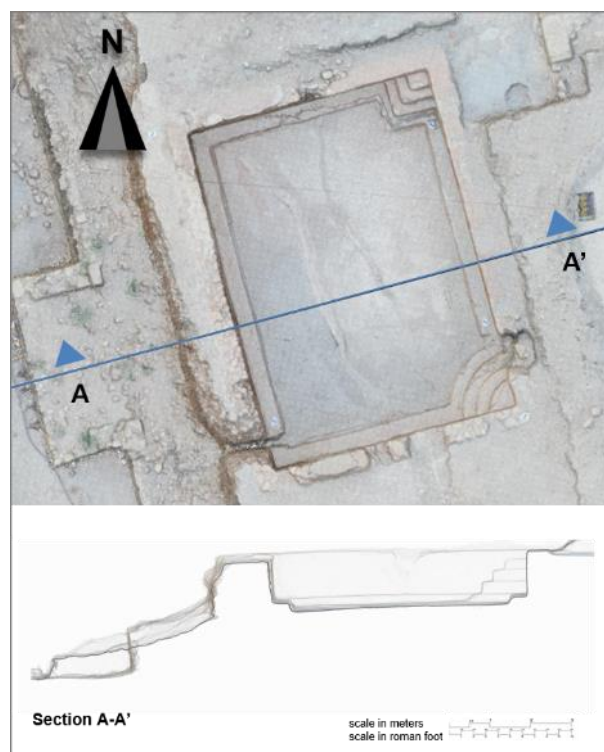

Figure 3: Orthophoto of the natatio at the Western Baths, the remains of the buttress of the rectangular wall can be seen on the left. A cross section is included.

dominated the *frigidarium*, a room of considerable dimensions and partially excavated which occupied a good part of the thermal space between the heated rooms of the east and the closing wall of the west. This great open room may have had some porticoed sections in the connecting areas with adjacent rooms.

This space would have an optimal area for outdoor exercise, complementary to the use of the thermal baths. The excellent orientation of the building and in particular of the frigidarium, open to the west, would guarantee a greater luminosity and solar heat for the users (Vitruvio, *De arch.* V, 10 & 11; VI, 1).

Research findings suggest that the base of the *natatio* began to crack at an imprecise moment, but in any case, before the end of the third century[2]. Archaeologically, different fractures are detected in the western half of the vessel, with a north-south direction that disperses towards the west. There are various repairs and patches characterized by contributions of ash deposited in the fractures and covered by thick layers of *opus signinum*. The depth of the base of the pool would have been altered resulting in the affected half tilting westward. This likely led to the opening of a second evacuation point near the southwestern corner.

The *natatio* stopped functioning at the baths in the late 3rd or early 4th century after undergoing continuous repairs. The site was later used as a landfill. The ash, from the cleaning of the furnaces that heated the adjacent rooms or from the construction elements discarded in punctual repairs of the building, was poured into the *natatio* basin. This archaeological data points to a continuity in the use of the baths during the 4th century despite the impossibility of maintaining the pool as a bathing area.

1.2. LIDAR technology applied to the study of this *natatio*

It is widely agreed that LIDAR and photogrammetry techniques are very accurate and useful for the real graphic records of the construction (Boehler, Heinz & Marbs, 2002; Lerma, Cabrelles, López, Navarro, Seguí, 2013; Guidi et al., 2008). Point clouds and digital images, both in orthometric formats and in immersive 360º formats, can be used to document places with archaeological remains in three dimensions, as currently presented. Furthermore, this allows users to obtain evidence of its deformation and degradation with high precision (Gordon & Lichti, 2007; Ferrer, Gámiz & Reinoso, 2019; Torres-González, Cabrera & Calero-Castillo, 2023).

In our case, the different campaigns of archaeological work have been used for documentation since 2016 (the date when the Master Plan of the Site of La Alcudia was drawn up (Gutierrez & Louis, 2018), mainly to support the graphic document. Furthermore, and as part of the digital databases of the whole site, it gives us added value because it helps us to monitor and control the wall elements, their overall state and the evolution of their deformation and their degradation at the much larger and more specific scales for their coatings and finishes (Martinez, Abellan & Berrezueta, 2022).

2. Objectives and methodology

The main objective of this work is the study and analysis of the geometry and deformations of the *natatio* at the Western Baths of La Alcudia in Elche from three-dimensional digitalized data and the study of historical and constructive data.

The study of deformations is approached from two perspectives. On the one hand, the current deformation is obtained by comparing its shape (point clouds recorded in 2022) with hypothetical datum planes. On the other hand, the increase of deformations between 2016 and 2022 by comparison of clouds obtained with LIDAR is also studied (Fassi, Fregonese; Ackermann & Troia, 2013).

Hypotheses are developed regarding the appearance of cracks and the early abandonment of using this constructive element that was very important to the operation of the whole thermal baths.

At first glance, the materials of the *natatio* have been gradually degrading. Therefore, another objective of this work is the study of these degradations and their evolution from the data obtained in 2016 and 2022.

The methodology used has a multidisciplinary basis, combining historical and archaeological research with direct observation, digital recording of the construction and analysis of the constructive elements that make up the *natatio*.

In the documentary study, all the pre-existing information has been compiled, from that provided by the first studies at the end of the 19th century (Ibarra, 1926; Abad, 2012; Ronda, 2018) to the data obtained, with updated methodology, in recent archaeological excavations (Tendero & Ronda, 2013 & 2020; Tendero & González, 2021).

The survey of the *natatio*, from a constructive point of view, was carried out by carefully observing the different construction systems present on site. It has been completed by using archaeological methodology based on the relationships established between the stratigraphic units detected and the materials they contain. From this last perspective, the dates proposed in this work have been formulated.

The photos were taken with a Canon 80D digital SLR camera with 24.3 MP CMOS APS-C sensor and RGB+IR metering sensor with 7.560 pixel and ISO sensitivity of 100, using graphic reference scales. And also using a DJI drone model Mavic 2 Pro with 1" CMOS sensor 20 MP effective pixels, GPS + GLONASS, and lens FOV: 77° 35 mm equivalent format: 28 mm and aperture of f/2.8 - f/11 and focus distance: 1 m at ∞.

For the 3D geometrical survey, various tools have been used, such as the Terrestrial Laser Scanners (TLS) Leica BLK and Leica C10 with their corresponding integrated digital cameras, as well as the software for their registration, processing and analysis of the point clouds.

Both digital images using photogrammetric techniques and captures with TLS itself obtain point clouds with their real colour using specific software (Metashape by Agisoft[3]

---

[2] The archaeological material context of the abandonment of this structure dates back to the end of the 3rd century or the beginning of the following century.

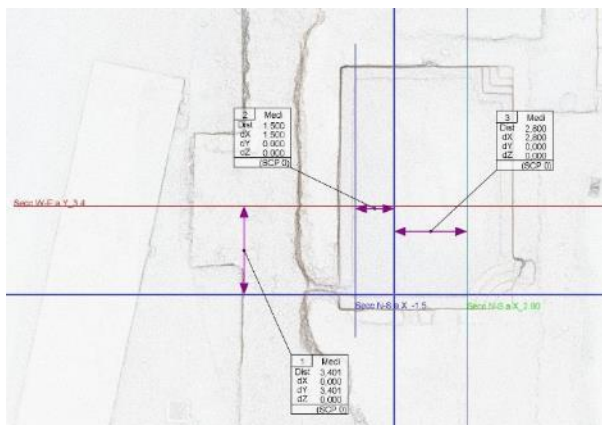[3] Metashaoe Professional Software (educational license) of Agisoft version 2.0.1.

Figure 4: Point cloud obtained from aerial photogrammetry. The section planes are indicated to obtain polylines in ACAD for deformation studies.
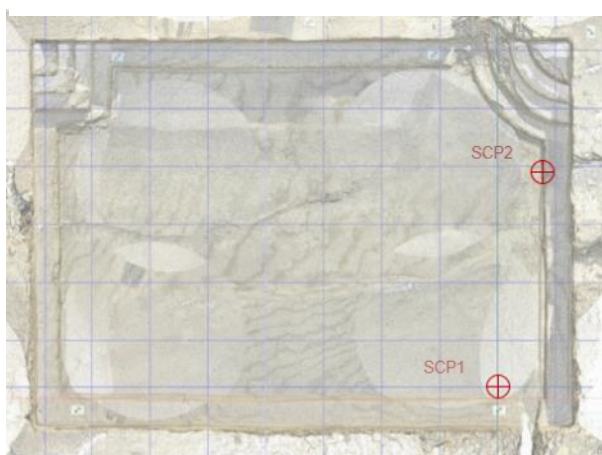

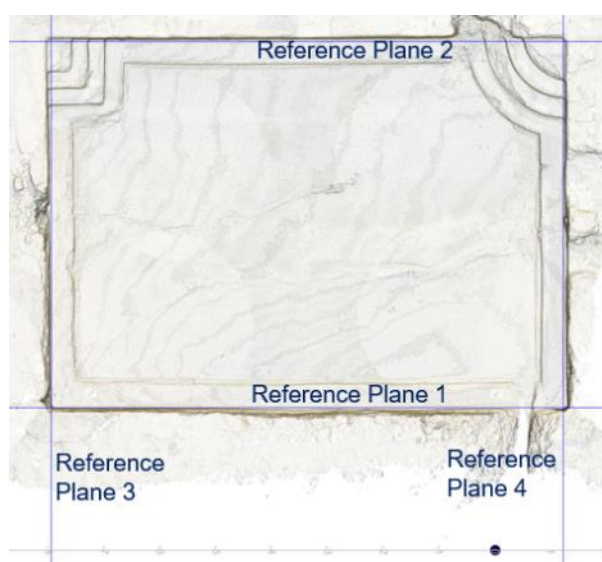**Figure 5:** Point cloud of the plan *natatio* with reference points.

Figure 6: Point cloud of the *natatio* in plan with lines with the reference plane in blue.

and Cyclone Register 360[4]). All the point clouds have been georeferenced from reference points located near the study area and obtained from the use of the GPS

Leica Viva GNSS with receiver GS08plus, with real-time satellite kinetic navigation system (GNSS with RTK), and controller CS10.

2.1. Methodology for deformation studies

The study of these deformations was based on the comparison of the actual geometry obtained at the end of 2022 (point cloud obtained by photogrammetry) with the ideal reference plans that they must have had originally, taking into account the good work of the Roman builders. That is vertical walls without deformations and the bottom of the *natatio* with uniform slopes towards the drain.

In this case, 3 section planes have been generated according to a reference origin (SCP0): 2 with North South orientation, initially parallel to the west and east walls, and 1 with W-E orientation perpendicular to the previous ones (Fig. 4).

Using sections of the point cloud, contours have been drawn in the form of polylines for the deformation control. By exporting them to ACAD v. 2023 de Autodesk, the planar deformations between the hypothetical value of origin (initial hypothetical dimensions of the *natatio*) and the current real one (see deformation results) are evaluated and quantified.

The side walls should have been vertical in origin while the bottom had an average slope of approximately 1.8% up to its drainage point. Other values obtained help us to corroborate the hypothesis of movements in terms of historical events based on the archaeological surveys.

In addition, using the point clouds obtained by a terrestrial laser scanner and Cyclone 3DR software, the comparative study of the *natatio* has been carried out by creating reference plans generated from the points of origin of partial coordinates that coincide with the nearest points of lower elevation and the point of water evacuation of the *natatio* (SCP1 and SCP2), considering the main point SCP1 as the main point of the *natatio* (Fig. 5).

Globally, with the 2022 point cloud, and using the Cyclone 3DR tool, these deformations are identified and quantified thanks to a map with a colour scale of each of the interior elevations and the bottom of the pool. For the elaboration of these maps, reference planes ZX and ZY have been used (parallel to those that identify SCP1 and very close to the elevations to be studied identified as reference planes 1, 2, 3 and 4). This view of the complex, provides evidence for the hypothesis of the events surrounding its construction, use and phases of renovation (Fig. 6).

2.2. Methodology for the study of deformation and degradation increase

The study of the increase in deformation and degradation was based on the comparative study of point clouds obtained by terrestrial laser scanning (TLS) taken 6 years apart. These dimensional variations between clouds obtained in 2016 and 2022 provide valuable information on their degradation over time, with relevant data for their conservation and maintenance. CloudCompare[5] software and the Leica Cyclone 3DR have been used for this purpose.

---

[4] Leica Geosystem Cyclone Register 360+ software (educational license) version 2023.0.1

[5] Software CloudCompare licensed under GNU GPL (General Public Licence) version 2.12.4 (Kyiv) download at www.cloudcompare.org

The study has been approached in two different and complementary ways. On the one hand, the degradations of each wall were studied separately by obtaining the distance between the inner surface of the *natatio* and a parallel reference plane. In this way, images with colour gradients have been obtained depending on the distance of each point from the reference plane. On the other hand, a comparison of the surfaces has been made by overlaying the point clouds.

It should be noted that in order to scan the *natatio*, the mud deposits accumulated on the bottom were removed in order to avoid errors in the reading of the results. However, in 2016 the scanning was carried out after a period of rain that favoured the existence of plants, while the second scanning was carried out in December 2022 and there was no vegetation. In 2022, accumulations of detritus were observed on the surface of the running step at the bottom of the *natatio* due to disaggregations of the vertical faces. This data will be taken into account in the discussion of results, as well as the point density of each of the clouds (Fig. 7).

(a)   (b)

Figure 7: Control data and properties of the 2016 (a) and 2022 (b) point clouds.

A first phase of this study consisted in aligning the two clouds in order to be able to compare them. To do this, it was essential to generate the cloud-to-cloud model with the best possible accuracy and quality. Three random and visible points of both clouds were located as common reference points, in order to proceed to their alignment and coupling with the least possible error in this transformation (Fig. 8).

For this cloud alignment transformation, it was important to identify both the coupling points and to have high quality and high density clouds in order to obtain acceptable errors. After the alignment process, the RMSE obtained was around 5 mm using Cyclone 3DR (Fig. 9) and 7 mm using Cloud Compare (Fig. 10).

In the following phase, the comparative process between these clouds was carried out, obtaining interesting results, such as the loss of material in coating layers, washing and disintegration processes in areas of punctual runoff, loss of support layers and deformations of historical repairs.

3. The *natatio* at the Western Baths of La Alcudia

A *natatio* stored water and therefore had to be waterproof. Its construction elements had to be strong enough to withstand the water pressure on its walls and at its base without creating deformations that could fracture the basin. In addition, the water had to drain from the lowest point of the base.

(a)   (b)
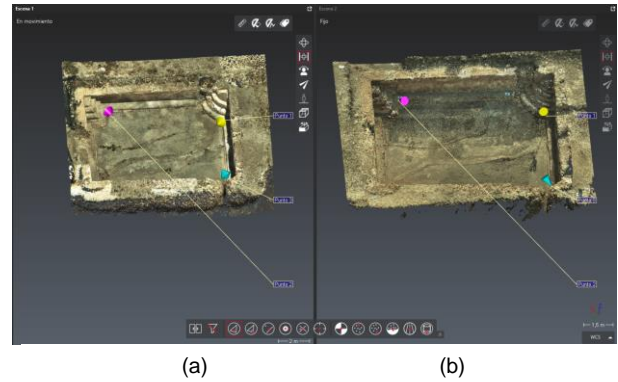
Figure 8: Points for the alignment of the point clouds: a) performed at the end of 2016; b) performed in 2022.
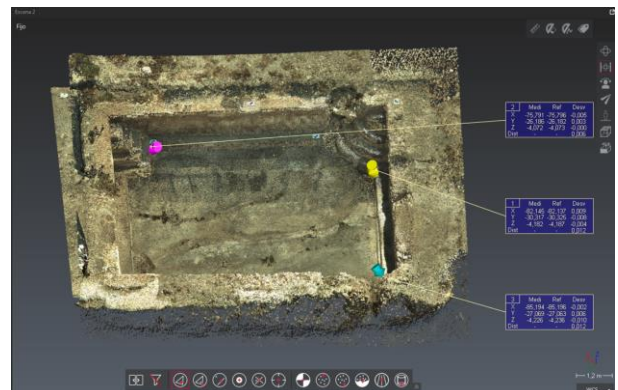
Figure 9: Cloud alignment with Cyclone 3DR.

Figure 10: Point cloud alignment using CloudCompare: a) Points measured for the alignment; b) final result.

The Romans were experts in water treatment, transport, and storage. Furthermore, they mastered the art of making waterproof mortars (Dilaria et al., 2022). They used layers of *opus signinum* cladding adding elements such as volcanic ash, crushed terracotta or vegetable ash to improve sealing (Lancaster, 2019).

3.1. Analysis of proportions (the Roman foot and the width, length, and depth) of wall thicknesses.

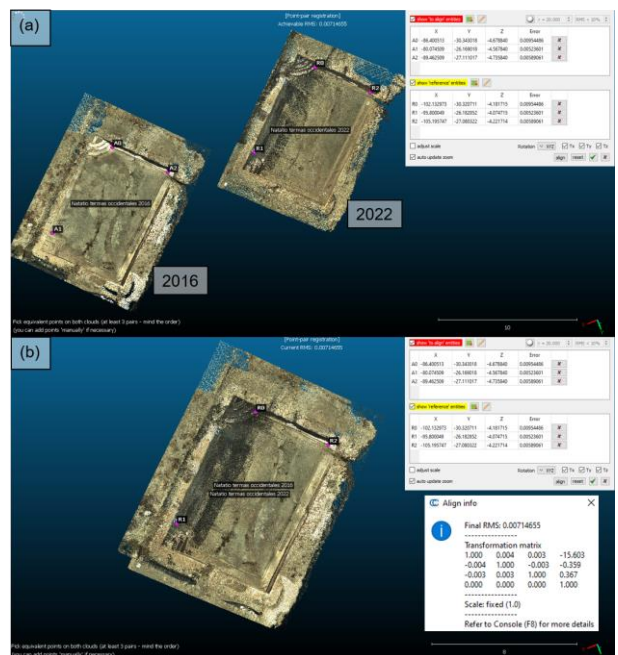The dimensions of the *natatio* basin, 6.60 x 9.30 m and 1.50 m deep, correspond to multiples or dividers of 30 cm (22 x 31 x 5 Roman feet). The studies currently being carried out in the Western Baths indicate that the Roman foot corresponds to 30 cm, unlike the 29.6 cm or 29 cm of other site areas (Molina, Álvarez & Muñoz, 2018).

The proportions of the sides of the rectangle of the *natatio* correspond to √2, as seen in Fig. 11, a typical design in some Roman constructions (Vitruvio, 2000; Esteban, 2001). The hypothetical shape of the original *natatio* is also shown in Fig. 11 in green.

Figure 11: Proportion study. The green line corresponds to the dimensions of the hypothetical original *natatio* area and the red lines to the current *natatio*.

The supporting structure of the walls is masonry of different thicknesses depending on the orientation. The narrowest is the one located to the east, approximately 2 Roman feet (60 cm), while that located to the north and south measures about (160 cm), and the western wall is much thicker (175 cm). This structure served to withstand the pressure of both the soil and the water in the basin. The *natatio* was lined inside with *opus signinum* with an average thickness of approximately 0.15 Roman feet (4.5-5 cm), which waterproofed the two layers of mortar. A lime whitewash acted as a surface finish.

3.2. The construction of the *natatio*

The *natatio* of the *Ilici* Western Baths was built on a heterogeneous foundation. The eastern half, which corresponds to the original *natatio*, rests on the wall and intramural levels of the city. The western half, which corresponds to the expanded section, rests on land filling the resulting the gap between the old city limit and the new western wall. That wall delimited the building and projected outside the walls to gain urban space.

The construction data differentiates between the western and eastern half of the *natatio* so each zone will be analysed separately.

Typical of the period, both natural stone (calcarenite and limestone) found close to the site and artificial stone (*opus caementicium, opus signinum* and lime grout) were used in its construction.

3.2.1. Wall located in the east and the eastern half of the north and south walls, corresponding to the original *natatio*

The foundation characteristics of this area still need to be explored due to the absence of archaeological surveys. However, the layout of the original wall had to pass under the original *natatio* constituting its foundation.

The cavity in the wall located to the east has allowed us to observe that it is 50-60 cm thick. It is built with medium-sized stones (between 10 and 40 cm) with abundant grip mortar. The masonry has been placed faceted, forming a reasonably regular wall that serves as the structure (Figure 12). The natural stones are mainly calcarenites, beige in colour and fixed with lime mortar. The wall had to be executed without formwork, ordering the stones manually.
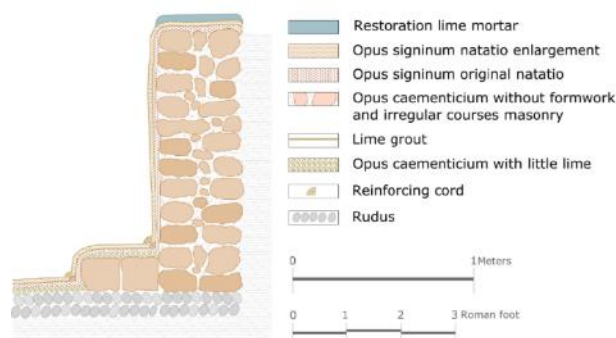
Figure 12: East *natatio* wall section drawing.

3.2.2. West wall and the western half of the north and south walls, corresponding to the extension of the *natatio*

The exterior of the west wall has been exposed due to landslides from the filling of the expanded space. This has allowed us to obtain more accurate data and to observe the differences both in the structure and in the materials used in its construction with regard to the eastern half (Fig. 13).

Figure 13: Photography of the back of the East wall. The rudus, the calcarenite blocks and the masonry of the wall are observed.

Figure 14: East *natatio* wall section drawing.

The archaeological sequence indicates that in the part of the filling that fills the space between the old wall line and the new work that delimited the baths to the west, there is a *rudus* or foundation preparation, consisting of pebbles of fluvial origin arranged mostly inclined (Fig. 14).

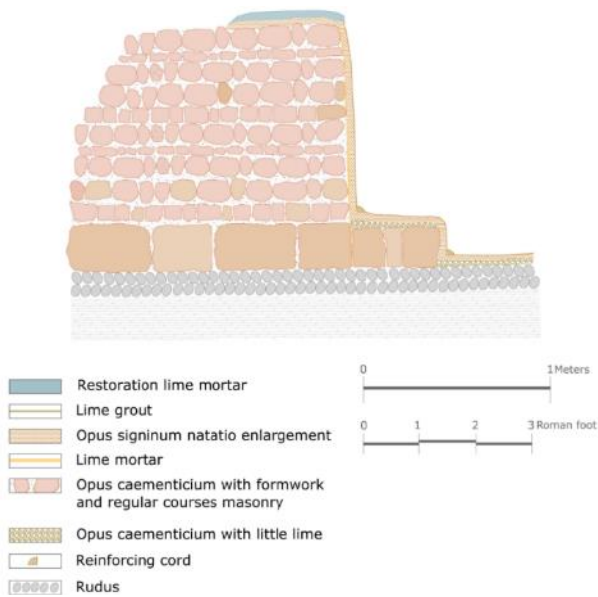On them, roughly carved quadrangular calcarenite stones are arranged. A wall of successive alternating lime mortar and limestone rests on this foundation, some with a particular inclination and resting on each other, forming a *pseudo-spicatum*.

The mortar is made from lime, sand, ash, and abundant pebbles (black, yellowish, whitish, and ochre) of fluvial origin. The stones are of a medium and small size, irregular, angular and with prominent edges, where reddish conglomerates abound. Both beds, mortar, and stone, have a comparable thickness of approximately 20 cm, so it has been assumed that a wooden formwork must have been used for their construction. Analysing some fractured or eroded points of the pool and its surroundings allows us to appreciate a global thickness of this core greater than 1.75 m in some areas.

Once the walls that make up the western half of the *natatio* have set, they are covered with a layer of *opus caementicium*, a mortar like substance used on these eastern walls; *opus signinum,* although a higher content of lime can be assumed as it is whiter in colour. A final coating of *opus signinum* was applied on top. In some areas, it was applied in two layers, this was a common practice in coatings greater than 2 cm thick to avoid avoiding generating cracks in the mortar. In the middle of the north wall, the transition between both types of coatings can be seen (Fig. 15). This layer forms a continuous plaster on the inside of the basin. Finally, a lime whitewash with ash is applied to improve its impermeability.

This *opus signinum* coating with grout is the same for the entire structure of the *natatio*, including the base. It is identified with the second layer detected in the eastern half previously described. With this coating, the overall finish of the *natatio* is unified, and subsequent repairs of fractures and deteriorated areas were made using *opus signinum* mortar.
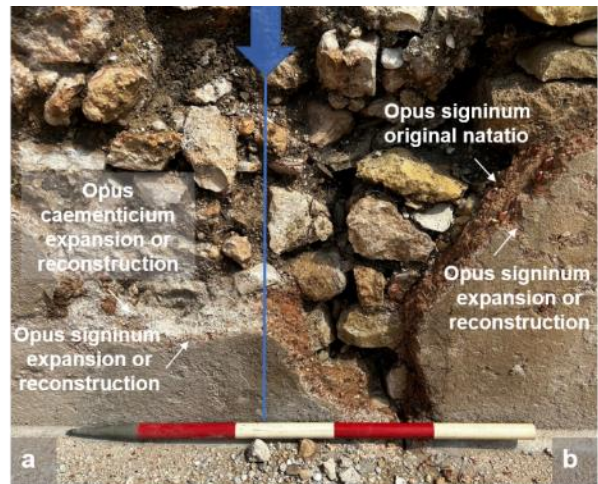

Figure 15: Photo of the north wall. The difference between coating mortars is observed: a) Extended *natatio*. b) Original *natatio*.

These walls have a first layer of plaster with *opus signinum* that also provides a finish for the perimeter projection of the *natatio* parapet. A delicate whitewash of lime with ashes preserves this layer, and a second layer of *opus signinum* is superimposed on the extension or reconstruction of the *natatio*, of a similar thickness to the first. After excavation in 2012, restoration mortar was placed on the top parapet to prevent leaks.

3.2.3. Interior of the *natatio*

Access to the interior of the *natatio* was gained via two stairways located at the northeast and southeast corners, respectively. The first has three quadrangular steps, and the second, another three in the shape of an arc or segment of a circle. In the lowest area, a fourth step was added, which served as a continuous bench that circled the perimeter of the basin.

The contact areas between the two stairs and the walls and the continuous bench at the base were reinforced with *opus signinum* in the form of a quarter-circle hydraulic cord. The presence of some fractures in the *natatio* has allowed us to observe these joints in detail Figures 12 and 14.

Observing the hollow next to the curved staircase has helped identify the different construction phases of the steps. The steps in the southeast corner are attached to the first *opus signinum* plaster, so they must have been built later than those in the northeast corner.

The core of these stairways also exhibits differences. The quadrangular steps were built with limestone, some carved in the shape of a parallelepiped (ashlars), joined with a light lime mortar. The curved steps have reddish conglomerates and irregular stones of a similar composition to the elements used in the walls of the western half, bound together with a more abundant mortar. A layer of *opus caementicium* with a low proportion of lime is deposited on the structure of all the steps and, on top, another layer of *opus signinum*. However, this last layer is double on the quadrangular stairs, an argument that reinforces the hypothesis that they were built in a previous phase. The last *opus signinum* layer also coats the *natatio*, creating a continuous waterproof layer reinforced at the vertical joints with hydraulic *signinum* cords. The bottom is at the same level as the foundation level of the wall of the western half of the *natatio* (Fig. 14).

Lastly, various elements are related to the collection and outlet of the water in the *natatio*. On the northern parapet, an interruption of the *opus signinum* of the coating can be detected, forming a channel 6 cm wide (1/5 Roman foot) (Fig. 16). It is possible that a pipe was housed in this crevice through which water was supplied to the basin. Subsequently, the channel is filled with a different mortar, blocking this supposed water entrance. At the base of the southern wall, in front of the aforementioned channel, there is a circular drain, 12 cm in diameter (2/5 Roman feet), where a lead pipe is housed. Its position suggests that it communicated with a section of the internal sewage pipes of the city excavated a little further to the south.

Figure 16: Photo of the north wall parapet. Semi-cylindrical hole 6cm in diameter filled with mortar is observed.

Next to the southwest corner, interrupting both the western wall and the continuous step of the base, a second drainage channel opens that crosses the entire wall and probably served to house a pipe to release water outside the walls. This second channel must have been built at a later time, so it was not part of the original construction of the *natatio*. It was part of the remodelling undertaken to solve the problems of the tilting of the base after its construction, fracture and damage.

4. Deformations and degradations of the *natatio*

It is necessary to know the state of conservation of the archaeological remains because when they are excavated, the humidity and temperature conditions change. They go from being in constant conditions and protected by the earth to being subjected to the elements and atmospheric agents. This tends to produce a gradual degradation, especially in areas where humidity is present (Rosina, Sansonetti, & Ludwig, 2018) and with the presence of salts (Grossi & Esbert, 1994). In the case of the *natatio*, the thrusts to which the walls are subjected have also been modified, as only one side of the walls is excavated. The absence of water inside the walls does not counteract the horizontal thrusts. In order to prevent the gradual degradation of the excavated remains, it is common practice to cover the archaeological remains and protect them from the weather. Obviously, this means that they cannot be observed or enhanced. The *natatio* was left exposed and unprotected after its excavation 10 years ago.

This building has several deformations and fractures. Some cracks were repaired with *opus signinum* as early as the Roman period. These cracks were sealed by slightly protruding from the surface of the bottom of the *natatio* (Fig. 17). In order to determine the possible causes of the movements, which in turn led to the cracks,

a detailed study of the current geometry of the *natatio* has been carried out, taking into account the historical evolution of this construction and its surroundings.

Damage can also be seen in all the walls of the *natatio*, especially the loss of material in the internal walls (masonry structure) and in the cladding. Detritus is continually falling off and accumulating in the surrounding areas. Figure 17 shows material detached and accumulated on the continuous step and on the bottom of the *natatio*. The picture also shows the cracks sealed with signinum.

Figure 17: Appearance of the bottom of the *natatio* with cracks sealed with *Opus Signinum* creating a curved ledge. Photo taken in December 2022.

In the study of deformation and degradation in this work, the terms included in the glossary on stone deterioration patterns (ICOMOS-ISCS, 2008) are used. This glossary refers to natural stone, but in this work it has been considered that they can be extrapolated to damage in artificial stone, considering that the petrophysical behaviour of natural and artificial stone is similar. According to the concepts and terms of the glossary, the problems and injuries present in the *natatio* have been classified in the following sub-sections:

- 1. Crack & deformation
- 2. Detachment
- 3. Features induced by material loss
- 4. Discolouration & deposit
- 5. Biological colonization

4.1. Crack & deformation

The study of the deformations begins by analysing the overall geometric form of the *natatio* today and comparing it with the hypothetical original form it must have had (Fig. 18). The premises that have been established from the outset consider that the side walls should be vertical and the bottom should have a certain slope towards the drain, which must have been the lowest point of the complex.

The *natatio* has a slope of 1.8% towards the main drain located to the south (SCP2). Subsequently, it was deformed and the lowest point became the southwest corner (SCP1), so they had to open another drain in that area. To create a steeper slope, they had to raise the bottom slightly. It can be seen that the base sealing string on the east bank is not parallel to the bottom in that part of the *natatio*.

In section "C" (Fig. 18d), a differential settlement and overturning of the *natatio* in a westerly direction can be observed. An 8º turn of the west wall and a settlement of 21.9 cm has been quantified in the section studied, which coincides with the lowest area at present on the west side. The highest point of the bottom is in the northeast corner. These deformations caused the cracks that fractured the *natatio* vessel longitudinally.

Longitudinal sections "A" and "B" (Figures 18b and 18c) show differential settlement in the central area of both sections. In section "A", located in the original area of the *natatio*, there is 5.3 cm of settlement, and the north and south walls show no deformation. In section "B", there is 8.7 cm of settlement with respect to the reference slope line at the bottom and the south wall has overturned outwards by 3º. It should be noted that the detachment of cladding has been taken into account, as this can distort the results.

4.2. Detachment

Detachment has been detected in all the natural (limestone rocks) and artificial (*opus signinum* and *opus caementicium*) stone materials that make up the *natatio*. Surface detachments of part of the material have occurred as a result of degradation. Exfoliations have been found, separating the materials by layers, between layers of cladding and in some of the natural stone that make up the structure that supports the *natatio*.

Damage is caused by disintegration of the natural or artificial stone into grains or clasts, which can affect the entire thickness of the stone material or only the surface (Grossi & Esbert, 1994). In the case of the *natatio*, numerous granular disintegrations have been observed. It has also occurred in the mortars of *opus caementicium, opus signinum* and in their finish as can be seen in Fig. 19. When the damage is reiterative, it ends up causing a significant loss of material.

4.3. Features induced by material loss

The main types of degradation affecting the *natatio* materials are found in this section. There are areas with severe detachment, especially due to erosion from the continuous passage of runoff water.

It should be noted that the presence of salts is a risk factor that gradually degrades natural and artificial stone materials. Salts are transported by water that is introduced into the capillary network of porous materials in accordance with Jurin's law and by osmotic effect, among other physical phenomena (Benavente, García-del-Cura, Fort, & Ordóñez, 2004).

Surface degradations have been observed as alveolizations. These cavities have been caused by the loss of material produced by haloclasty when water containing dissolved salts evaporates and crystallises, causing great pressures capable of fracturing natural and artificial stone materials (Rodriguez-Navarro & Dohene, 1999; Charola, 2000). When these degradations occur repeatedly, they end up causing high losses of material.

4.4. Discolouration & deposit

This section includes superficial alterations that affect the "skin" of the stone materials of the *natatio*. The main damages of this type are: efflorescence, discolourations, dirt deposits and natural patinas. The chromatic changes
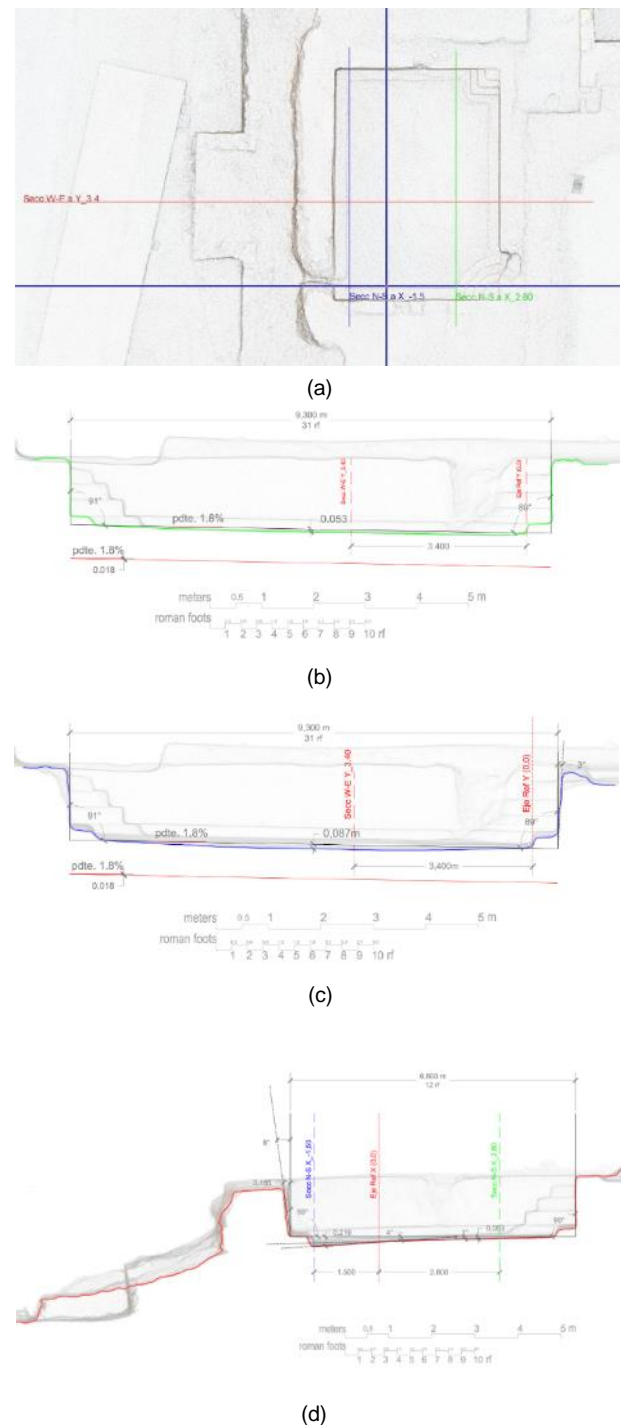
(a)

(b)

(c)

(d)

Figure 18: Plan and sections of the natatio drawn on a point cloud. Reference axes and section cut plans are included: a) Plan with section plans indicated; b) Section "A" North Southdirection in green colour next to steps; c) Section "B" North Southdirection in blue colour; d) Section "C" West Eastdirection in red colour.

due to biodeterioration are studied in the following section according to the classification established in the glossary on stone deterioration patterns (2008).

Efflorescences are whitish stains (Fig. 19a) due to the formation of soluble salt crystals. They are not very consistent and are usually produced on the surface of porous stone, due to migration and evaporation phenomena of water containing soluble salts.

The salts can come from different sources: from the composition of the materials themselves, from adjacent soils or even from bird droppings. A certain chromatic alteration has been detected in the surface colour of the stone. It has been observed that in the *natatio* there are modifications of the colour in the areas especially affected by humidity and sunlight.

The presence of some deposits of dirt due to the accumulation of material of various origins (dust, earth, soot, guano, micro-organisms, etc.) on the surface of the stone materials has been observed. They normally have low cohesion, variable thickness and low adherence to the substrate on which they are laid.

4.5. Biological colonization

Moisture retained in the pores and cavities of natural and man-made stone materials has led to the emergence and development of living organisms capable of generating biological colonization (Warscheid & Braams, 2000). Higher plants have roots that generate mechanical stresses, while lower plants such as lichens, mosses, algae and fungi especially cause harmful chemical actions by acidifying, among other actions, the area where they proliferate. When the disturbance is widespread, large "patches" of biopatina or biofilm are created. In the affected areas, a biofilm capable of penetrating and degrading several millimetres into the stone is produced (De los Ríos et al., 2009). In Figure 19b a biopatine coating zone is numbered as (6).

In the case of the *natatio*, there are materials of a carbonate nature that are particularly susceptible to the action of acids. These are most of the natural stones that make up the masonry, the mortars of *opus caementicium* and the limestone grouts of surface finish.

It has been observed that there is a greater or lesser presence of rooted plants in the *natatio* depending on the time of year, and especially on rainfall.
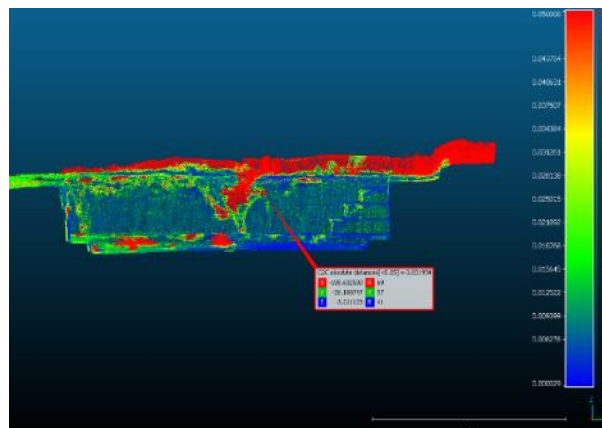

Figure 20: Comparison of 2016 and 2022 point clouds of the northern face of the natatio. Matching points are shown in blue, the other colours indicate geometrical differences between the compared clouds.

4.6. Study of deformations and degradations from the digitisation of the *natatio*

Figures 20 to 32 show the graphic studies of the degradations and deformations of the *natatio*. In the interpretation of the results, it should be taken into account that the cracks were sealed by creating a curved projection (Fig. 17), so that anomalies in the background plane appear in the point clouds in these areas. It must also be considered that the environment of the *natatio* has been modified with accumulations of earth generating anomalies (shown in red in Figures 20, 24, 27, 30 and 31 that show the superposition of the point clouds).

The study is approached by different faces, carrying out the study of point clouds with a colour gradient depending on the distance between the scanned surface and the reference plane in each case. The analysis of the superimposition of point clouds is also included.
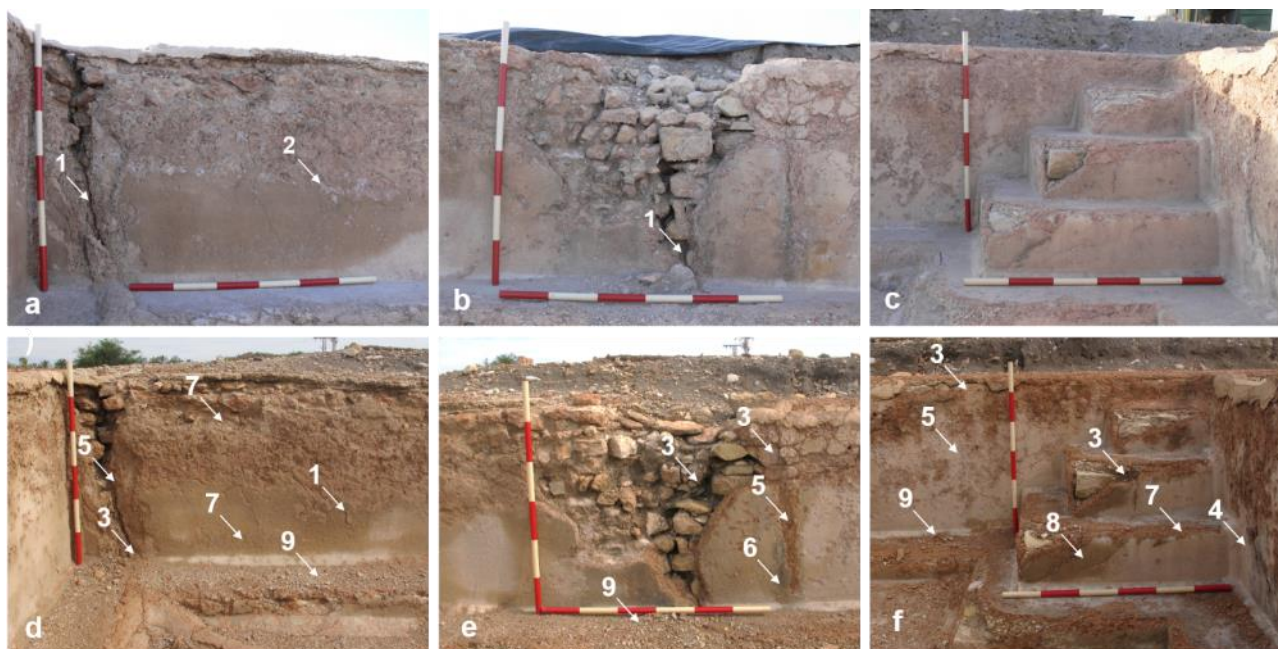

Figure 19: Different aspects of the north wall. Pictures a), b) and c) from the year 2016, photos d), e) and f) are from 2022. The following damages are indicated: 1.- Crack, 2.- Efflorescence, 3.- Detachment, 4.- Exfoliation, 5.- Erosion, 6.- Biological colonization, 7.- Granular disintegration, 8.- Discolouration, 9.- Stone and mortar detritus.
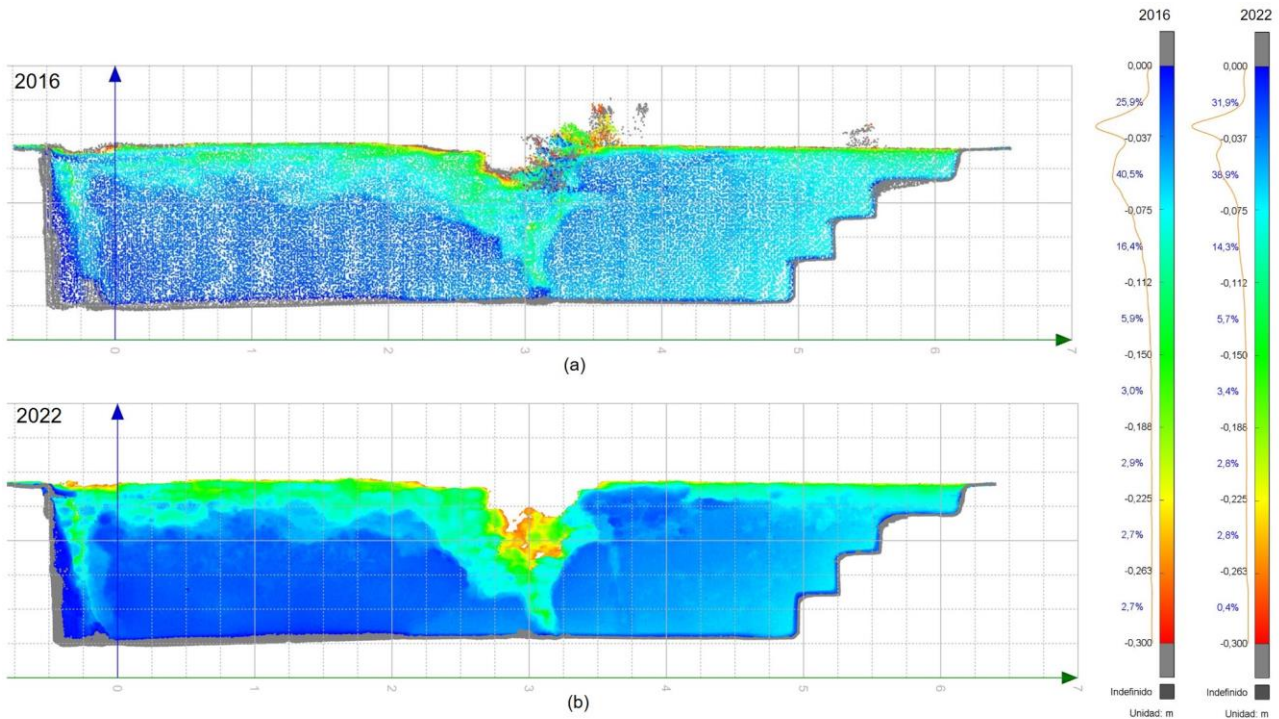
Figure 21: Point clouds with colour gradient as a function of distance from the reference plane 3 shown in Figure 5. The blue colours indicate closeness to the reference plane. On the right-hand side are the scales of each cloud with the percentage curve of points contained in the distances marked on the scale; a) Point cloud obtained in spring 2016; b) Point cloud obtained in December 2022; c) Point cloud obtained in December 2022; d) Point cloud obtained in December 2022.

In general, it can be seen that the original *natatio* has hardly been deformed. The enlarged/reconstructed area shows a differentiated settlement with a twist in the base and in the vertical faces towards the southwest corner.

4.6.1. Deformations and degradations on the north wall of the *natatio*

The study of the current deformations of the north wall shows that in general this wall has broken in two areas and has tilted to the west. There has been a differential settlement quantified at 19.2 cm. This deformation was measured in the lower part of the wall. It should be taken into account that the original drainage of the wall is located in the south wall and therefore the base of the north wall, under study in this section, should be completely horizontal.

Regarding the degradations, by analysing the colour gradients that represent the difference between reference plane 3 and the point clouds (Fig. 21), the degradations or loss of material can be clearly appreciated. Fig. 21a has less point density than Fig. 21b and is therefore less sharp in appearance, but it is still possible to assess the differences between clouds. The areas with colours other than dark blue correspond to detachments of the *opus signinum*. The colours from green to red indicate damage to the base wall of the *natatio.*

Figs. 20 and 21 show an increase in the loss of material in the fractures and in the area around the top of the *natatio*. There is also loss of *opus signinum* lining in the area next to the central hollow. The crack in the NW corner has also widened slightly.

The point cloud for 2022 shows 31.9% of the surface in blue, and for 2016, 25.9% according to the point distribution graphs in Fig. 21. In principle, if the wall had not been deformed, this should not be the case, since the cladding has been detached from 2016 to 2022. What this indicates is that the outer surface of the cladding is deforming towards the interior of the *natatio*. It can be seen that this area has less distance to the reference plane, with the dots in deeper blue.

Fig. 20 has been inspected in detail in the areas where the greatest deterioration has been observed. As an example, when the green coloured point located in the central area of the wall is studied, the difference between the point clouds of 2016 and 2022 is 3.19 cm (always taking into account the estimated RMSE of 0.7 cm). In situ, it has been observed that in this area the outer layer of the cladding has peeled off, the thickness of which is approx. 2.5 cm. The lower area has also deteriorated.

4.6.2. Deformations and degradations on the east wall of the *natatio*

This wall does not show serious deformations nor degradations except for the area with serious loss of material next to the curved stairs (Fig. 22) where there has been a high loss of material. It should be noted that the cavity allows the entry of rainwater through runoff that carries material even from the walls of the *natatio* itself.

This facing is the one with the largest area of *opus signinum* cladding and lime grout finish. A comparison of the point clouds in Figs. 23a and 23b shows few differences in the distance from the reference plane. The 2022 point cloud shows more points closer to the

Figure 22: Appearance of the east wall next to the staircase in the southeast corner in 2022.
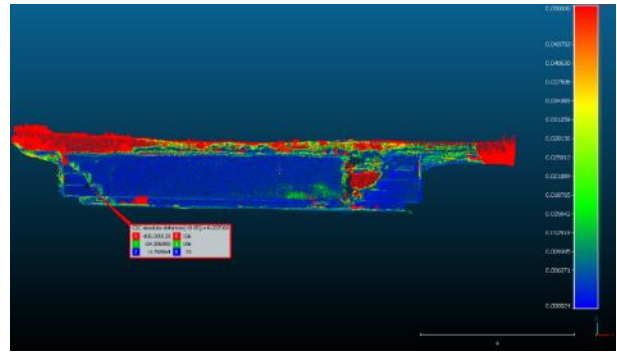

Figure 24: Comparison of 2016 and 2022 point clouds from the east. Matching points are shown in blue, the other colours indicate geometrical differences between the compared clouds. The environment of the natatio has been modified by generating noise in red.
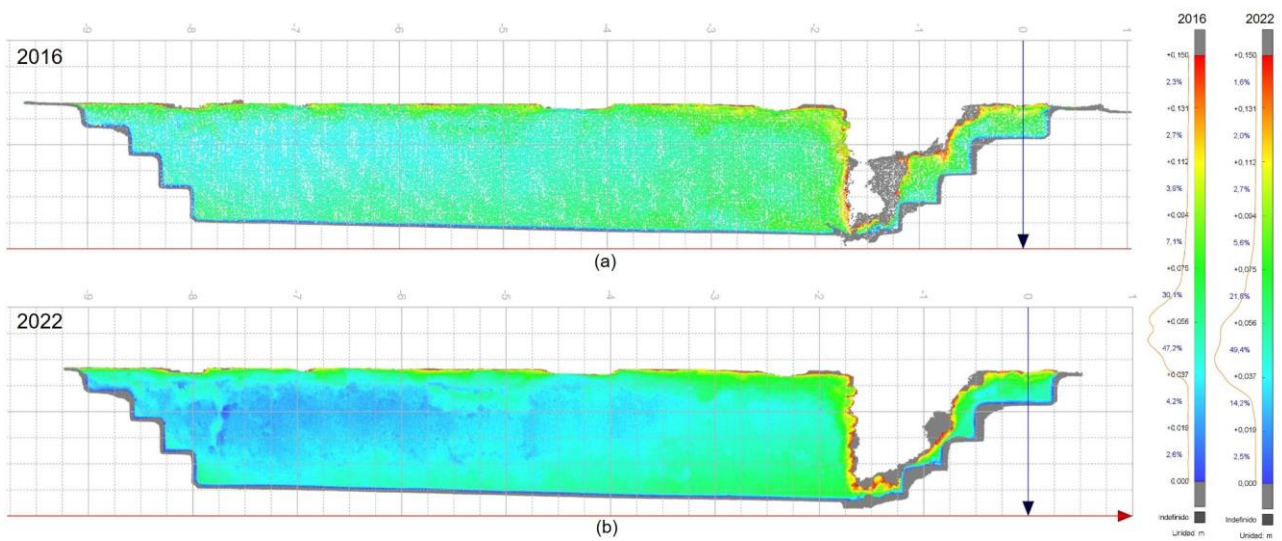

Figure 23: Study of the surface of the facing to the east of the *natatio*. Colour gradient as a function of distance from reference plane 2 (Figure 5). The points in blue are those close to the cutting plane: a) surface in the year 2016; b) surface in the year 2022. Differences are observed between the two point clouds due to increased degradations.

reference plane. In the 2022 point cloud, 66,1%[6] of the surface is blue, and the 2016 cloud contains 54.5%[7]. It should be noted that in the 2022 cloud an area of cladding next to the south staircase has disappeared. This shows that the cladding is degrading and separating from the base by displacement. This damage has been indicated in Fig. 19f.

The cloud comparison in Fig. 24 shows the increased loss of material in the fracture (evident from visual inspection (Fig. 22).

The edges of the stairs also show degradations which are shown in green in Fig. 24 where, as an example, the deformation data of the 3rd rectangular step is included. The difference at that point between 2016 and 2022 point clouds is 3.7 cm (always taking into account the estimated RMSE of 0.7 cm). In situ, it has been observed that in this area the outer layer of the cladding has detached, the thickness of which is approx. 2.8 cm. This damage can be seen in Fig. 19f.

Figure 25: Appearance of the southern face in the year 2022.

---

[6] Percentage adding the 2.5 deep blue, the 14.2 blue and the 49.4 light blue according to the Figure 24 dot plots.

[7] Percentage adding the 2.6 deep blue, the 4.2 blue and the 47.7 light blue according to the Figure 24 dot plots.

4.6.3. Deformations and degradations on the south face of the *natatio*

This wall shows a fracture in the centre where the wall turns toward the south and a differential settlement between the east and west sides (Fig. 25). In the upper zone of the fracture, material has been lost from both the supporting wall and the cladding. There is loss of cladding material especially in the upper areas of the wall.

Figure 25 shows that the western half of the fracture is further away from the reference plane, which is why the dots are in green. This is due to the wall facing the south.

With regard to the study of the evolution of damage between 2016 and 2022, the comparison of the point clouds in Fig. 26 shows an increase in the loss of material, especially in the central fracture zone. Part of the lining has been lost in the upper zones. This damage is also reflected in Fig. 27. The central crack shown in this figure has opened 1.4 ± 0.7 cm at the measured point. This does not imply that the walls have been displaced, as this may be due to the passage of runoff water.

In the year 2022 there are fewer points close to the reference plane (Fig. 26b). In this point cloud, 3.2% of the surface area appears in deep blue, whereas the 2016 cloud contains 6%. This is evidence of the detachment of the coatings.

4.6.4. Deformations and degradations on the west wall of the *natatio*

This wall shows numerous deformations and degradations. There is a high loss of part of the wall in the southern corner with a fracture that cuts through to the base of the wall (Fig. 28).

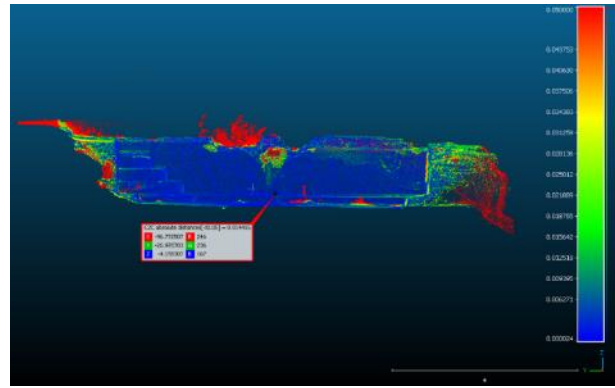**Figure 27:** Point cloud overlay of the south wall in 2016 and 2022.

Figure 28: Appearance of the west face in the year 2022. Indicated as "1" is the arch-shaped discharge saddle. A recent crack is indicated as "2".
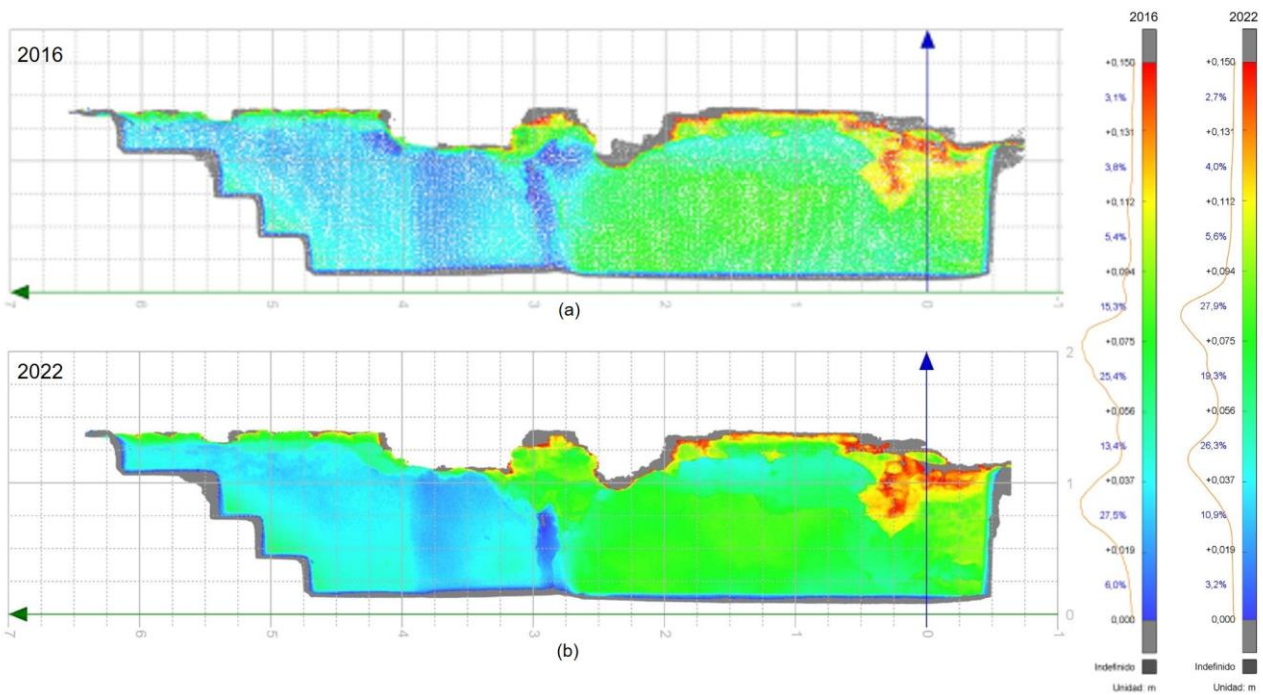

Figure 26: Study of the surface of the southern face of the *natatio*. Colour gradient as a function of distance from reference plane 4 (Figure 5); a) year 2016; b) year 2022.
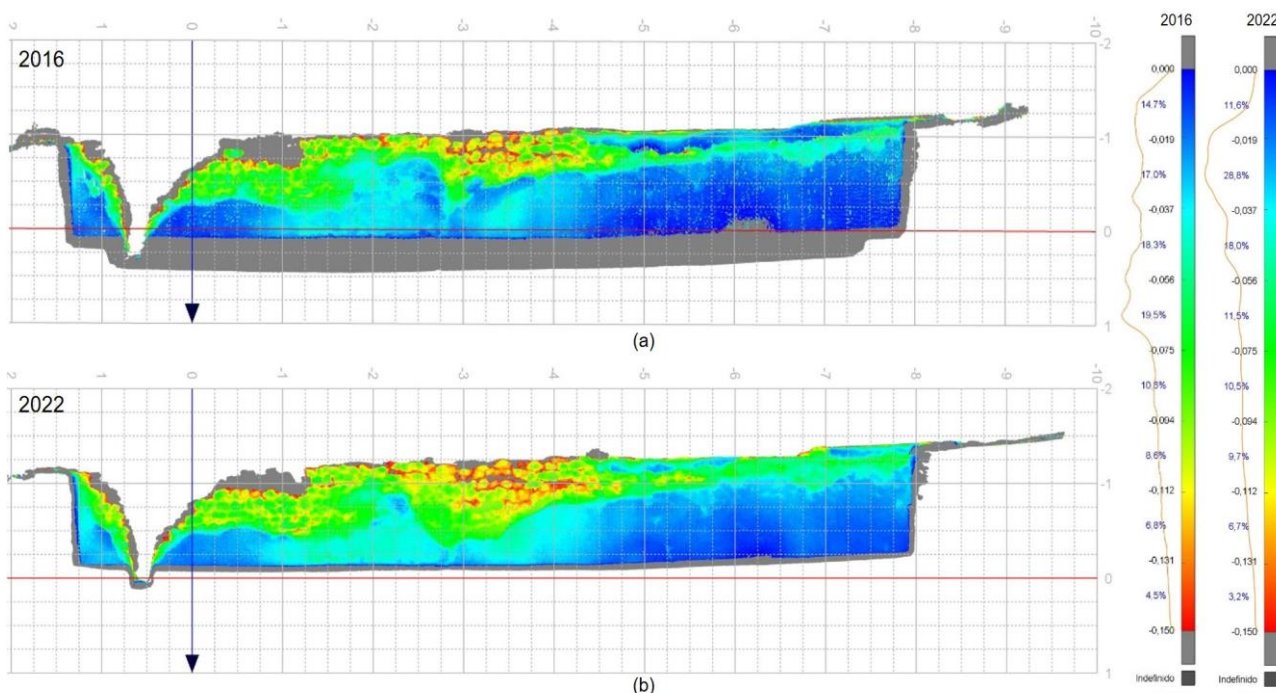
Figure 29: Survey of the werstern facing *natatio*. Colour gradient as a function of distance from reference plane 1 (Fig. 5): a) year 2016; b) year 2022.
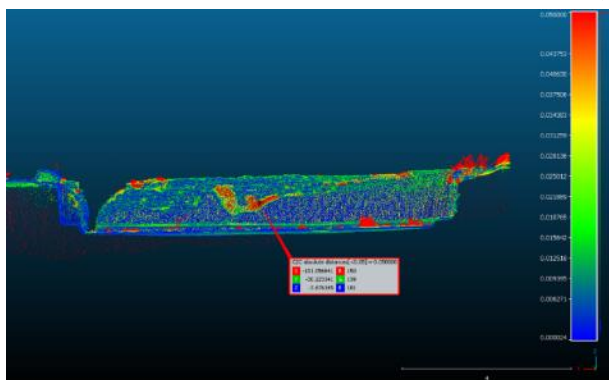

Figure 30: Overlay of 2016 and 2022 point clouds of the west facing *natatio*.

Figure 31: Comparison of point clouds for the year 2016 and 2022 of the bottom of the *natatio*. Matching points are shown in blue, all other colours imply changes in the geometry of the *natatio*. The red colour indicates differences greater than 5 cm.

The entire wall is slightly turned to the west and in the centre contains a relief arch, indicated as "1" in Fig. 29. There is a high loss of facing material, especially in the upper areas of the wall. Regarding the study of the evolution of damage between 2016 and 2022, the comparative point clouds in Fig. 29a show a high increase of material loss in the central zone. Material has been lost in the upper zones. This damage is also reflected in Fig. 30, which shows that in the central area in red the loss of material exceeds 5 ± 0.7 cm. The crack indicated as "2" in Fig. 28 is shown in red in Fig. 30.

The 2022 cloud contains fewer points close to the reference plane (Fig. 29b). In the 2022 point cloud, 11.6% of the surface is deep blue, while the 2016 cloud contains 14.7%. This is evidence of the detachment of the coatings. The matching points appear in blue, the other colours indicate geometrical differences between the clouds compared. In 2016 there were plants generating red anomalies in the background of the *natatio*. In general, surface degradations are observed. In the centre of the facing there are red areas indicating detachments of the *opus signinum* cladding. Fragments have broken off in the upper left area.
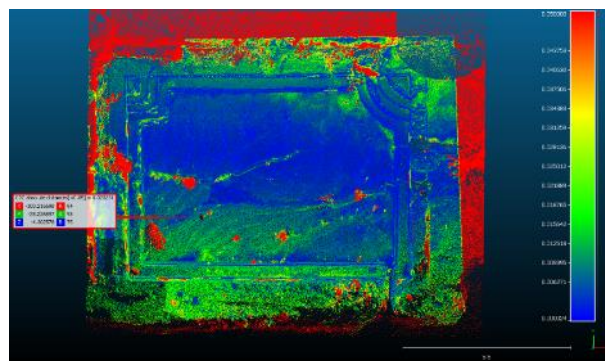
4.6.5. Deformations and degradations on the bottom of the *natatio*

The bottom of the *natatio* is severely deformed. This is clearly shown in Figs. 31 and 32. The gradient of colours according to the distance from the reference plane facilitates the observation of the differential settlement of the *natatio* towards the southwest.

A horizontal plane at -20 cm from the point SCP1 (Fig. 5), located at the lowest part of the base of the *natatio*, is taken as a reference plane. As concluded from the point cloud study, the southwest corner is 28 cm below the northeast corner. On the other hand, in the north-east corner under the stairs, detritus from nearby cladding detachments has accumulated, which also generates orange anomalies (Fig. 32).

The original drain is located in the area indicated as "1" in Fig. 32a. In this area, it can be seen how the slope of the bottom was increased to facilitate the evacuation of the water. The average slope has been quantified at approx.
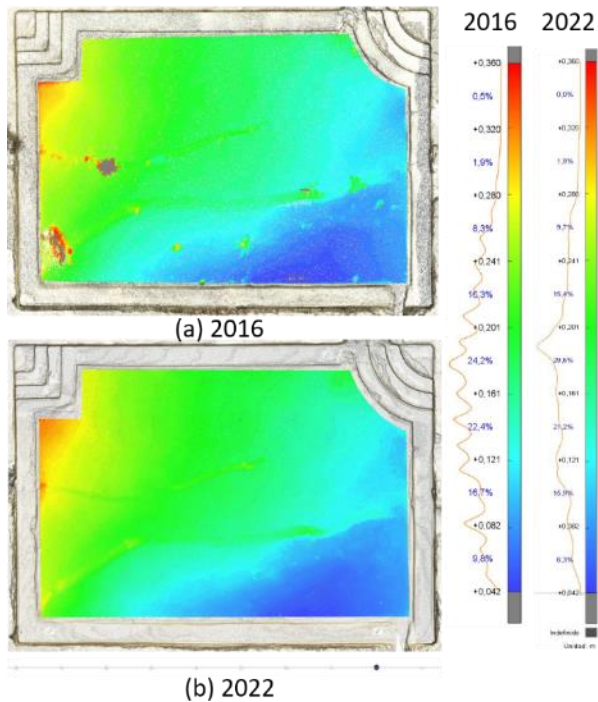
Figure 32: Background study of the natatio. Colour gradient as a function of distance from the reference plane: a) year 2016; b) year 2022.

1.8% in the eastern part of the *natatio,* which coincides with the original *natatio*. Therefore, the eastern half of the *natatio* has hardly suffered any deformation. In this case, the study of point clouds for 2016 and 2022 (Fig. 32), hardly provide any information due to the wide range (31.8 cm from + 0.042 m to + 0.36 m) that had to be used to obtain data for the entire background.

Even so, small differences can be seen in the northwest area, which are much clearer in Fig. 31. In this comparative study, differential deformations can be seen in green, in the western area of the bottom, which corresponds to the unloading arch of the western wall, studied in section 4.6.4. Also the northwest corner shows increases in deformation.

5. Discussion

5.1. Discussion of methodology

Regarding the methodology used in the comparison of point clouds for the degradations study, it should be noted that point clouds have been obtained with different levels of definition. The laser scanning carried out in 2016 was part of the total scan of the site and was performed with a lower density of points than the scan of 2022. This last scan was performed exclusively to study current deformations and see the progress of degradations; therefore, it was made with greater density of points. This situation is not ideal for this type of comparative work, since it can lead to greater inaccuracies in the results. The overlay of point clouds using the CloudCompare software automatically gives more error (12 mm) than making an evaluation by picking points manually (7 mm), these points, according to in situ observation and photographic information, have not been altered.

The discussion of results should consider anomalies due to the uneven growth of vegetation in the *natatio* and accumulations of earth and occasional landslides in the environment of the *natatio* that has changed over the years. In the study of point clouds with respect to a reference plane, the maximum distance of interest must be well-tested so that the range (distance between blue and red points) is not very large, because information is lost. This was the case for the study of the bottom of the *natatio*, where the differential settlement has made it necessary to put a range of 31.8 cm.

Furthermore, point cloud analysis and processing assessed the different types of materials that comprise the *natatio*. The coatings of bearing walls are easily discernible, providing information about their thickness.

5.2. Discussion of constructive evolution

The analysis of the geometry of the *natatio*, together with the data extracted from the archaeological surveys, offer the following constructive serialization:

- Phase I. Construction phase dated during the Flavian dynasty, in the last quarter of the 1st century (Tendero & Ronda, 2020). The original *natatio*, preserved today in the eastern half of the current structure, is equipped with an access stairway in the northeast corner, a feeding channel on the north parapet and its outlet in the South wall.

- Phase II. Between its construction and an indeterminate moment in the 2nd and 3rd centuries. The construction of the *natatio* is modified by expanding or rebuilding half of the pool to the west. The curved stairway of the southeast corner is built. The construction elements of phase I (quadrangular stairs and drainage of the south wall) are still in operation. The whole complex is unified with the same *opus signinum* coating.

- Phase III. Dated between Phase II and the end of the 3rd century. Deformations, fractures and cracks. Patches and repairs. Opening of the second drain. We do not rule out that these structural deformations are related to the high seismic activity found in other southern Hispano-Roman cities, such as Carthago Nova, Corduba or Baelo Claudia, at the beginning of the second half of the 3rd century (Quevedo & Ramallo, 2015; Ruiz, 2017; Morín de Pablos et al., 2014; Silva et al., 2016).

- Phase IV. Dating from the end of the 3rd or beginning of the 4th century to the beginning of the 5th century. Abandonment of the *natatio* as a space for bathing. The basin is used as a landfill for thermal waste. The rest of the Western Baths are still in operation.

- Phase V. Dated in the 5th century and following centuries. The filling in of the basin of the *natatio* with urban waste and remains of fragmented construction materials resulting from looting. Definitive abandonment of the building as a thermal space. Slow clogging of the *natatio* until it is level with the surrounding land during the 6th to 10th centuries.

5.3. Discussion of deformation study

The results obtained allow us to quantify the deformations of the *natatio* (with an error of approximately 5 mm) when making the comparison with the hypothetical original shape of each face (estimating that originally the side walls were vertical, and the bottom had a slope of 1.8%).

The fractures suffered by the *natatio* have openings that are greater than 5 cm in some areas, which show that the movements that caused them were elevated. The most likely source of such deformations, which led to a crack along the pool basin, are differential settlements produced by the western half of the pool on landfill between the two walls. The tilting of the pool towards the southwest would have led to the creation of the second drain, which poured water directly to the west side. This drain caused possible sinkage in the foundation, which increased deformation and, consequently, would generate more cracks. Fractures could also be sources of water leakage that, in turn, were generating greater differential settlements at the bottom. The land where the pool was built has now countless sinkholes attributed to ground water erosion, due to leaks of rainwater that wash the ground gradually. A comparative analysis of the geometry of the *natatio* between 2016 and 2022 suggests that there have been slight changes in the W half of the *natatio*, both at the base and on the walls. The central crack that cuts the *natatio* basin in two and reaches the south wall has increased by about 1.6 ± 0.5 cm. The bottom and inner continuous bench in the western half has been deformed by about 2 ± 0.5 cm on average. The difference between the bottom of the *natatio* in 2016 and 2022 has been quantified in 2.3 ± 0.7 cm. This is an indication that there is some active differential settlement in this area.

5.4. Discussion of the degradation of the *natatio*

Regarding the degradation of the walls, it has been observed that there has been a worrying increase from 2016 to the present day. The areas next to holes and cracks are particularly damaged due to erosion by water runoff. The stairs also show great deterioration. In general, all the walls have increased damage. Wall cladding has undergone granular disintegration and the finishing lime milk has been partially removed.

In N elevation, the central sinkhole of the wall, where the rainwater flows, has experienced an increase in material loss. The rainwater comes from accumulation in the upper bench and then enters the *natatio.*

In E elevation, increased damage is lower than in the other, although superficial detachments have been observed, mainly in the lime milk on the *opus signinum* and in the hollow next to the stairway.

The S elevation currently shows areas of *opus signinum* coatings completely detached and a higher surface degradation in comparison with 2016.

The W wall has lost a lot of facing and finishing material. In the analysis of degradation factors for the *natatio* materials, both extrinsic degradation agents to which the materials are exposed and changes in environmental conditions must be taken into account.

The design mission of the *natatio* was to contain water, and the materials used for its construction were resistant to the action of water and generated a waterproofing of the pool. Nowadays, however, the *natatio* no longer holds any water and it is surrounded by soil, which retains moisture and salts. This moisture is transferred by capillary action to the walls and cladding, where it is exposed to the atmosphere. For this reason, the humidity and temperature conditions have changed. The *opus signinum* and its protective lime milk are therefore exposed to continuous wet and dry cycles of humidity with a certain salt content. According to several studies (Zhou et al., 2018; Zhang et al., 2021; Meng et al., 2023; Benavente, Martínez-Martínez, Cueto, & García-del-Cura, 2007), these actions reduce mechanical strength by increasing the porosity of both natural and artificial stone materials.

According to numerous authors (Cardell et al., 2003; Benavente, Cultrone & Gómez-Heras, 2008; Benavente, De Jongh & Cañaveras, 2021) and others, the crystallisation of salts accelerates the disintegration of clasts and compounds, causing a continuous granular disintegration over time in the crystallisation zone due to the effect of crystallisation pressures. In addition, salts are highly hygroscopic, meaning that they can absorb water vapour and cause the substances in which they are incorporated, to attract more water through osmotic action. It has been observed that the presence of saline efflorescence coincides with the most granular disintegrated areas. Furthermore, the effect of rainfall with the presence of wind increases the effect of degradation on stone materials (López-González, Gomez-Heras, Otero-Ortiz, Garcia-Morales & Fort, 2022).

Regarding the methodology of the comparative study between point clouds, it has been shown that the non-existence of fixed points of reference in the environment of the *natatio* has generated a possible average error of 7 mm. For this reason, for similar future projects, fixed reference points should be located in areas close to the element under study and, if possible, within the *natatio*. Such locations should not be subject to possible deformation or degradation. The results indicate active movement and degradation in the *natatio* which must be taken into consideration when planning possible stabilization actions. Preventive maintenance is necessary to avoid water entering the interior of the *natation.* Research must be monitored and progressed in order to protect this built heritage.

6. Conclusions

The study and treatment of the data provided by the point clouds obtained by LIDAR, together with the collection, study and analysis of documentary data, has increased our knowledge of the area of the Western Baths at the archaeological site of La Alcudia in Elche.

This work concludes that there are two perfectly differentiated parts and that they coincide exactly with half of the current *natatio*. The measurements of the original preserved area are 3.30 m by 9.30 m (11 x 31 Roman feet 30 cm). The historical and construction data point to an expansion of the *natatio* although it is possible that the western half collapsed and this would lead to its partial reconstruction. The extended or reconstructed area doubles the measurements of the preserved original area. The *natatio* currently measures 6.60 m x 9.30 m (subtracting deformations), corresponding to a length width ratio of √2.

From a construction perspective, this study has made it possible to show that the eastern part of the *natatio* is covered with two layers of *opus signinum* (one per phase), and its masonry walls are made up of beige limestone and sandstone. However, the part added to the west is covered with a single layer of *opus signinum* on thicker expansive walls, made up of alternating reddish limestone stones and thick beds of *opus caementicium* built with formwork. As we have already seen, these differences are also extrapolated to the corner stairs, which justifies their assignment to different construction phases.

The land on which they built the extension of the *natatio* on the outside of the wall was a mixture of soil and stones, which caused differential settlements. The deformations caused changes in the slopes at the bottom and an overturning of the west wall, with the appearance of several cracks that affected the entire *natatio* basin. These fractures were sealed with *opus signinum*, mortar commonly used as a waterproof coating. The deformations have required another drain to be opened in the southwest corner, coinciding with the lowest point.

The superimposition of the point clouds taken in 2016 and 2022 shows that there are currently increases in degradation and deformation.

Regarding the degradation of the surface and even the shape of the walls, it has been verified that there is a worrying increase in degradation, especially significant in the N, S and W faces of the *natatio*, in addition to the area with water leaks next to the curved stairway on the wall located to the E. The restoration mortar placed to prevent leaks on the horizontal top of the walls has become detached.

It can be affirmed that the origin of the increase in degradation is due mainly to the erosion caused by runoff water and the exposure to meteorological agents aggravated by the crystallization of salts on the surface of the walls. This data allows us to predict the possible evolution of the degradation of the construction elements studied; the point clouds obtained will also serve as a reference for future studies.

In conclusion, this work demonstrates the importance of addressing interdisciplinary studies for optimal knowledge of ancient construction remains and their conservation. Analysis from different perspectives resolves unknowns that would not be possible from a single focal point. In the same way, this interdisciplinary approach opens up new working hypotheses that must be addressed in the future, with the planning of specific explanatory archaeological surveys.

Acknowledgements

References

Abad Casal, L. (2012). Pedro Ibarra y el descubrimiento de las Termas Occidentales en La Alcudia de Elche. In J. M. Abascal, A. Ceballos, S. Castellanos & J. Santos (Eds.), *Estudios de Historia Antigua, Homenaje al profesor Manuel Abilio Rabanal,* (pp. 249-274). León-Sevilla: Universidad de León & Universidad de Sevilla.

Abad Casal, L., & Tendero Porras, M. (2008). *Ilici. La Alcudia de Elche. Guía del parque arqueológico.* Fundación Universitaria de Investigación Arqueológica La Alcudia.

Alföldy, G. (2003): Administración, urbanización, instituciones, vida pública y orden social. In J. M. Abascal & L. Abad Casal (Eds.), *Las ciudades y los campos de Alicante en época romana. Canelobre, 48* (pp. 35-57). Alicante: Instituto de Cultura Juan Gil-Albert.

Álvarez Tortosa, J. F., Molina Vidal, J., & Muñoz Ojeda, F. J. (2020). Las Termas Orientales de La Alcudia (Elche, Alicante). Nuevos resultados de la campaña de excavación 2018. In M. Ponce, F.E. Tendero, Y. Alamar & Ll. Alapont (Coords.), *Jornades d'arqueologia de la Comunitat Valenciana: 2016-2017-2018* (pp.189-194). Valencia: Generalitat Valenciana, Direcció General de Cultura i Patrimoni, Conselleria d'Educació, Cultura i Esport.

Benavente, D., Cultrone, G., & Gómez-Heras, M. (2008). The combined influence of mineralogical, hygric and thermal properties on the durability of porous building stones. *European Journal of Mineralogy*, *20*(4), 673–685. https://doi.org/10.1127/0935-1221/2008/0020-1850

Benavente, D., García-del-Cura, M. A., Fort, R., & Ordóñez, S. (2004). Durability estimation of porous building stones from pore structure and strength. *Engineering Geology, 74*(1-2), 113–127. https://doi.org/10.1016/j.enggeo.2004.03.005

Benavente, D., Martínez-Martínez, J., Cueto, N., & García-del-Cura, M. A. (2007). Salt weathering in dual-porosity building dolostones. *Engineering Geology, 94*(3-4), 215–226. https://doi.org/10.1016/j.enggeo.2007.08.003

Benavente, D., de Jongh, M., & Cañaveras, J. C. (2021). Weathering processes and mechanisms caused by capillary waters and pigeon droppings on porous limestones. *Minerals*, *11*(1), 18. https://doi.org/10.3390/min11010018

Boehler, W., Heinz, G., & Marbs, A. (2002). The potential of non-contact close range laser scanners for cultural heritage recording. *International Archives of Photogrammetry Remote Sensing and Spatial Information Sciences*, *34*(5/C7), 430-436. https://www.isprs.org/PROCEEDINGS/XXXIV/5-C7/pdf/2001-11-wb01.pdf

Cardell, C., Delalieux, F., Roumpopoulos, K., Moropoulou, A., Auger, F., & Van Grieken, R. (2003). Salt-induced decay in calcareous stone monuments and buildings in a marine environment in SW France. *Construction and Building Materials*, *17*(3), 165-179. https://doi.org/10.1016/S0950-0618(02)00104-6

Charola, E. (2000). Sales in the Deterioration of Porous Materials: An Overview. *Journal of the American Institute for Conservation*, *39*(3), 327-343. https://doi.org/10.2307/3179977

De los Ríos, A., Cámara, B., García del Cura, M. A., Rico, V. J., Galván, V., & Ascaso, C. (2009). Deteriorating effects of lichen and microbial colonization of carbonate building rocks in the Romanesque churches of Segovia (Spain). *Science of the Total Environment*, *407*(3), 1123-1134. https://doi.org/10.1016/j.scitotenv.2008.09.042

Dilaria, S., Secco, M., Rubinich, M., Bonetto J., Miriello, D., Barca, D., & Artioli, G. (2022). High-performing mortar-based materials from the late imperial baths of Aquileia: An outstanding example of Roman building tradition in Northern Italy. *Geoarchaeology*, *37*(4), 637–657. https://doi.org/10.1002/gea.21908

Esteban Lorente, J. F. (2001). La teoría de la proporción arquitectónica en Vitruvio. *Artigrama*, *16*, 229-256.

Fassi, F., Fregonese, L., Ackermann, S., & Troia, V. (2013). Comparison between laser scanning and automated 3D modelling techniques to reconstruct complex and extensive cultural heritage areas. *International Archives of the Photogrammetry, Remote Sensing and Spatial Information Sciences*, *XL-5/W1*, 73-80. https://doi.org/10.5194/isprsarchives-XL-5-W1-73-2013

Ferrer-Pérez-Blanco, I., Gámiz-Gordo A., & Reinoso-Gordo, J. F. (2019). New Drawings of the Alhambra: Deformations of Muqarnas in the Pendentives of the Sala de la Barca. *Sustainability, 11*(2), 316. https://doi.org/10.3390/su11020316

Gordon, S. J., & Lichti, D. D. (2007). Modeling terrestrial laser scanner data for precise structural deformation measurement. *Journal of Surveying Engineering*, *133*(2), 72-80. http://dx.doi.org/10.1061/(ASCE)0733-9453(2007)133:2(72)

Grossi, C. M., & Esbert, R. M. (1994). Las sales solubles en el deterioro de rocas monumentales. Revisión bibliográfica. *Materiales de Construcción*, *44*(235), 15-30. https://doi.org/10.3989/mc.1994.v44.i235

Guidi, G., Remondino, F., Russo, M., Rizzi, A., Voltolini, F., Menna, F., Francesco, F., Sebastiano, E., Masci, M. E., & Benedetti, B. (2008). A multi-resolution methodology for archeological survey: the Pompeii forum. In M. Ioannides, A. Addison, A. Georgopoulos & L. Kalisperis (Eds.), *Proceedings of the 14th International Conference on Virtual Systems and Multimedia (VSMM 2008)* (pp. 51-59). Limassol: Arqueolingua. http://diglib.eg.org/handle/10.2312/14806

Gutiérrez, S., & Louis Cereceda, M. (Coords.) (2018) L'Alcudia d'Elx. Plan director 2017-2029. Alicante: Servicio de Publicaciones Universidad de Alicante.

Ibarra Ruiz, P. (1926). *Elche. Materiales para su historia*. Cuenca: Talleres tipográficos Ruiz de Lara.

ICOMOS-ISCS (2008). *Illustrated glossary on stone deterioration patterns*. International Council on Monuments and Sites – International Scientific Committee for Stone. http://www.international.icomos.org/publications/monuments_and_sites/15/pdf/Monuments_and_Sites_15_ISCS_Glossary_Stone.pdf

Lancaster, L. C. (2019). Pozzolans in mortar in the Roman empire: An overview and thoughts on future work. In I. Fumadó Ortega & S. Bouffier (Eds.), *Mortierset hydraulique en Méditerranée antique, Archéologies Méditerranéennes,* (pp. 31-39). Aix-en-Provence: Presses Universitaires de Provence.

Lerma García, J. L., Cabrelles López, M., Navarro Tarín, S., & Seguí Gil, A. E. (2013). Modelado fotorrealístico 3D a partir de procesos fotogramétricos: láser escáner versus imagen digital. *Cuadernos de Arte Rupestre, 6*, 85-90.

López-González, L., Gomez-Heras, M, Otero-Ortiz de Cosca, R., Soledad Garcia-Morales, S., & Fort, R. (2022). Coupling electrical resistivity methods and GIS to evaluate the effect of historic building features on wetting dynamics during wind-driven rain spells. *Journal of Cultural Heritage*, *58*, 209-218. https://doi.org/10.1016/j.culher.2022.10.009

Martínez-Martínez, J., Abellán, A., & Berrezueta, E. (2022). Erosion directionality and seasonality study using the anisotropy matrix. Application in a semiarid Mediterranean climate (SE Spain). *Science of the Total Environment, 804*, 150165. https://doi.org/10.1016/j.scitotenv.2021.150165

Meng, J., Li, C, Zhou, J-Q., Zhang, Z., Yan, S., Zhang, Y., Huang, D., & Wang, G. (2023). Multiscale evolution mechanism of sandstone under wet-dry cycles of deionized water: From molecular scale to macroscopic scale. *Journal of Rock Mechanics and Geotechnical Engineering*, *15*(5), 1171-1185. https://doi.org/10.1016/j.jrmge.2022.10.008

Molina Vidal, J., Álvarez Tortosa, J. F., & Muñoz Ojeda, F. J. (2018). Arqueología y socialización del conocimiento en La Alcudia de Elche las Termas Orientales. In J. C. Márquez Villora, R. Navalón García & J. L. Soler Milla (Eds.), *El mundo del agua, paisaje de vida: Patrimonio histórico-cultural del Vinalopó* (pp. 197-208). Elda: Ayuntamiento. http://hdl.handle.net/10045/132815

Molina Vidal, J., Muñoz Ojeda, F. J., & Álvarez Tortosa, J. F. (2020). Las Termas Orientales de La Alcudia (Elche, Alicante): nuevas perspectivas de la investigación reciente (Proyecto Astero-UAPatrimonio Virtual). In J.M. Noguera, V. García-Entero, & M. Pavía (Coord.), *Termas públicas de Hispania. SPAL Monografías Arqueología, 33.* (pp. 471-480). Murcia/Sevilla: Ediciones de la Universidad de Murcia/Editorial Universidad de Sevilla.

Morillo Cerdán, A., Durán Cabello, R., & García Marcos, V. (2019). Las termas legionarias de León. Análisis e interpretación arqueológica de su ángulo sureste. *Zephyrus*, *83*, 107-138. https://doi.org/10.14201/zephyrus201983107138

Morín de Pablos, J., Silva, P. G., Rodríguez-Pascua, M. A., & Sánchez-Ramos, I. Mª (2014). Evidencias arqueosísmológicas en la Colonia Patricia de Córdoba (Valle del Guadalquivir, España). In J. A. Álvarez & F. Martín (Eds.), *Resúmenes de la 2ª Reunión Ibérica sobre fallas activas y paleosismología* (pp. 159-162). Lorca: Instituto Geológico y Minero de España.

Noguera, J. M., García-Entero, V., & Pavía. M. (Coords.) (2020). Termas públicas de Hispania. *SPAL Monografías Arqueología*, *33*. Murcia/Sevilla: Ediciones de la Universidad de Murcia/Editorial Universidad de Sevilla.

Quevedo Sanchez, A., & Ramallo Asensio, S. F. (2015). La dinámica evolutiva de *Cathago Nova* entre los siglos II y III. In L. Brassous & A. Quevedo Sánchez (Eds.), *Urbanisme civique en temps de crise: les espaces publics d'Hispanie et de l'Occident romain entre les IIe et IVe S.* (pp. 161-178). Madrid: Casa de Velazquez.

Ramos Fernández, R., & Ramos Molina, A. (2007). Las Termas Orientales de *Ilici. Caesaraugusta, 78*, 545-554.

Rodriguez-Navarro, C., & Dohene, E. (1999) Salt weathering: Influence of evaporation rate, supersaturation and crystallisation pattern. *Earth Surface Processes and Landforms*, *24*, 191–209.

Ronda Femenia, A. Mª. (2018). La Alcudia de Alejandro Ramos Folqués, contextos arqueológicos y humanos en el yacimiento de la Dama de Elche. Serie Arqueología. Alicante: Universidad de Alicante.

Rosina, E., Sansonetti, A., & Ludwig, N. (2018). Moisture: The problem that any conservator faced in his professional life, *Journal of Cultural Heritage*, *31*(Supplement), S1-S2, https://doi.org/10.1016/j.culher.2018.04.022

Ruiz Bueno, M. D. (2017): Actividad sísmica en el mediodía ibérico durante el siglo III d.C. La incidencia arqueológica en Corduba (Córdoba)*. Pyrenae, 48*(2)*,* 29-51. https://doi.org/10.1344/Pyrenae2017.vol48num2.2

Silva, P. G., Giner-Robles, J. L., Reicherter, K., Rodríguez-Pascua, M. A., Grützner, C., García Jiménez, I., Carrasco García, P., Bardaji, T., Santos, G., Roquero, J., Röth, J., Perucha, M., Pérez-López, R., Fernández Macarro, B., Martínez-Graña, A., Goy, J. L., & Zazo, C. (2016). Los terremotos antiguos del conjunto arqueológico romano de *Baelo Claudia* (Cádiz, Sur de España): quince años de investigación arqueosismológica. *Estudios Geológicos, 72*(1), e050. http://dx.doi.org/10.3989/egeol.42284.392

Tendero Porras, M., & González Ferré, D. (2021). Aproximación a las Termas Occidentales de *Ilici* a partir de sus materiales cerámicos de construcción. *Boletín del Museo Arqueológico Nacional, 40*, 129-145.

Tendero Porras, M., & Ramos Molina, A. (2014). El sector 4C de La Alcudia de Elche. MARQ, Arqueología y Museos, II Jornadas de arqueología y patrimonio alicantino. Arqueología en Alicante en la primera década del siglo XXI, extra-01, (pp. 240-246). Alicante: MARQ, Museo Arqueológico de Alicante.

Tendero Porras, M., & Ronda Femenia, A. Mª (2013). La ciudad romana de *Ilici* (L'Alcúdia de Elche, Alicante). In M. Olcina (Ed.), *Ciudades Romanas Valencianas* (pp. 226-242). Alicante: MARQ-Diputación de Alicante.

Tendero Porras, M., & Ronda Femenia, A. Mª (2020). Las Termas Occidentales de *Ilici*: redescubrimiento y nuevas aportaciones arqueológicas. In J.M. Noguera, V. García-Entero, & M. Pavía (Coord.): *Termas públicas de Hispania. SPAL Monografías Arqueología*, *33* (pp. 457-469). Murcia/Sevilla: Ediciones de la Universidad de Murcia/Editorial Universidad de Sevilla.

Torres-González, M., Cabrera Revuelta, E., & Calero-Castillo, A. I. (2023). Evaluación fotogramétrica del estado de degradación de los revestimientos decorativos: las yeserías del Patio de las Doncellas (Reales Alcázares de Sevilla). *Virtual Archaeology Review*, *14*(28), 110–123. https://doi.org/10.4995/var.2023.18647

Vitruvio Polión, M. L. (2000). *Los diez libros de arquitectura*. Barcelona: Iberia S.A.

Warscheid, Th., & Braams, J. (2000). Biodeterioration of stone: a review. *International Biodeterioration & Biodegradation*. *46*(4), 343-368. https://doi.org/10.1016/S0964-8305(00)00109-8

Zhang, Z., Niu, Y., Shang, X., Sí, P., Zhou, R., & Gao, F. (2021). Deterioration of Physical and Mechanical Properties of Rocks by Cyclic Drying and Wetting. *Geofluids*, 6661107, 1–15. https://doi.org/10.1155/2021/6661107

Zhou, Z., Cai, X., Ma, D., Chen, L., Wang, S., & Tan, L. (2018). Dynamic tensile properties of sandstone subjected to wetting and drying cycles, *Construction and Building Materials*, 182, 215-232. https://doi.org/10.1016/j.conbuildmat.2018.06.056